Effects of electron-phonon interaction on non-equilibrium transport through single-molecule transistor

Zuo-Zi Chen,[1, *] Rong Lü,[1] and Bang-fen Zhu[1, 2, †]

[1]*Center for Advanced Study, Tsinghua University, Beijing 100084, P. R. China*
[2]*Department of Physics, Tsinghua University, Beijing 100084, P. R. China*
(Dated: February 2, 2008)

On the basis of the nonequilibrium Green's function and nonperturbative canonical transformation for the local electron-phonon interaction (EPI), the quantum transport through a single-molecule transistor(SMT) has been investigated with a particular attention paid to the joint effect of the EPI and SMT-lead coupling on the spectral function and conductance. In addition to the usual EPI-induced renormalized effects (such as the red-shift, sharpening, and phonon-sidebands of the SMT level), owing to improved disentagling the electron-phonon system, it has been found that, the profile of the spectral function of the SMT electron is sensitive to lead chemical potentials, thus can readily be manipulated by tuning the bias as well as the SMT-gate voltage. As a consequence, the broken particle-hole symmetry in this system can be clearly recognized through the phonon sidebands in the spectral function. These EPI effects also manifest themselves in the nonequilibrium transport properties of the SMT, particularly at low temperature.

I. INTRODUCTION

With the remarkable advances in the ability to fabricate the nanostructures, it is possible to explore the electronic devices based on a single molecule, i. e. the single-molecular transistor (SMT),[1,2] which might promise to be potential candidates for nano-electronics and also provide with an controllable tool in studying the fundamental physics in nanometer scale.

It has been found that the transport through the single-molecular transistor might exhibit profound many-body correlated effects at low temperature, such as the Coulomb blockade or the Kondo effect.[1,3,4,5,6] An important feature for the SMT is its sensitivity to the local molecular vibration, which will have profound impacts on the transport properties.[2,7,8,9] This may also be true in some quantum dot(QD) systems whenever there is a strong coupling between the dot electron and local phonon mode. In addition, the SMT is usually connected to the outside gates via the leads. Since the applied bias voltage to the SMT is within nanometers, a small bias might cause to substantial field effect, thus the transport through a SMT or QD is in general a nonequilibrium process.

Theoretically, many efforts have been made towards the quantum transport through the SMT or QD with these features taken into proper account. Theoretical approaches developed in this field include the kinetic equation method,[10] the rate equation approach,[11,12] the nonequilibrium quantum theory,[13,14,15,16] and more recently the numerical renormalization group calculation.[17,18,19] In doing such investigations, several groups have already accounted for the electron-phonon interaction (EPI), many-body effects, or nonequilibrium properties.[12,20,21] However, different results may be obtained by different treatments of these effects.[12,16] Although the numerical renormal-

ization group method can well predict the equilibrium properties of the system, it cannot be applied to the nonequilibrium situation directly. While regarding to the present systems, a theory capable of dealing with both nonequilibrium and strong EPI situations should be favorite. One candidate, the Keldysh Green's function, has shown to be successful for the nonequilibrium systems.[22,23,24,25,26,27] Within this framework the nonequilibrium Dyson equations are solved self-consistently, in which the self energies due to the EPI can be calculated by the standard many-body diagrammatic technique,[22,23] or by using the self-consistent Born approximation.[24] Such an approach can meet the present concerns, and can be generalized to account for the effects arising from the phonon dynamics itself.[24] But, in general, the calculations are complicate as self-consistent integrals are encountered. This difficulty can be circumvented by directly diagonalizing the EPI terms with a canonical transformation,[28,29] as long as the phonons are in the thermodynamic equilibrium and the fluctuation in phonons can be neglected. By an improved treatment in the decoupling approximation as presented in the present work, which differs from the majority of previous publications,[16,28] the electron can be properly decoupled from phonon system, and yet permits to straightforward solutions in a compact, analytic form.

In this paper, by combining the nonequilibrium Keldysh Green's function technique with the canonical transformation for the electron-phonon system, we intend to study the quantum transport through the SMT in the presence of finite bias and strong local EPI, with special attention paid to the effect of the improved decoupling treatment for the electron-phonon system on the spectral function. The paper is organized as follows. In section II, an Anderson-Holstein model is introduced for the SMT in the presence of local EPI, then our main theoretical framework is described, in which the commonly
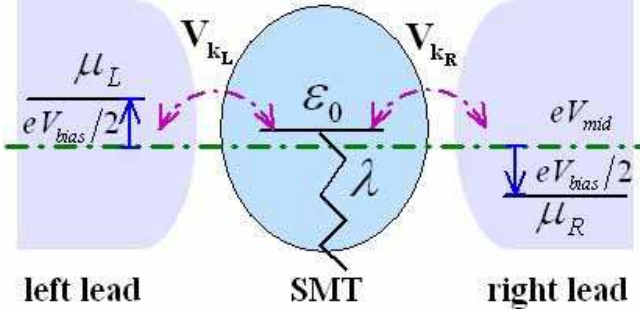
FIG. 1: Schematic illustration for the single-molecule transistor system.

used procedure for decoupling the electron-phonon system is carefully reexamined. In section III, the numerical results for the spectral function of the SMT electron is demonstrated and discussed, including both the dressing effects due to the EPI and the joint effects caused by its interplay with the SMT-leads coupling. An interesting phenomenon is predicted that the profile of the spectral function for the SMT electron can be manipulated at low temperature by tuning the chemical potentials in the leads. Consequently, the phonon sidebands in the spectral function may be quite asymmetric with respect to the renormalized SMT level, indicating a broken electron-hole symmetry. In section IV, it is shown how the effect of the different decoupling approximation on the spectral function manifests itself in the conductances of the SMT at zero temperature and finite temperatures, which might yield nearly the same results at high temperature, but definitely different behaviors at zero temperature. Finally, a brief conclusion is drawn.

II. PHYSICAL MODEL AND FORMALISM

A. Model

As shown in Fig.1, our model system is a single electron level in a SMT or QD, which is coupled to the local vibration mode as well as to two metallic leads. For the sake of simplicity, we shall restrict ourselves exclusively to the effect of the EPI and chemical potentials in two leads, thus ignore other factors, such as the intricacies of the real SMT, Coulomb interaction and spin effect. The model Hamiltonian can be then expressed as

$$\mathbf{H} = \mathbf{H}_{\text{leads}} + \mathbf{H}_{\text{ph}} + \mathbf{H}_{\text{D}} + \mathbf{H}_{\text{T}}, \tag{1}$$

where the first two terms of the Hamiltonian represent the noninteracting electron gas in the leads and the local vibration mode of the SMT, respectively, namely,

$$\mathbf{H}_{\text{leads}} = \sum_{\mathbf{k} \in L(R)} \epsilon_{\mathbf{k}} \mathbf{c}_{\mathbf{k}}^{\dagger} \mathbf{c}_{\mathbf{k}}, \qquad \mathbf{H}_{\text{ph}} = \omega_0 \mathbf{a}^{\dagger} \mathbf{a}. \tag{2}$$

Here the operator $\mathbf{c}_{\mathbf{k}}^{\dagger}$ ($\mathbf{c}_{\mathbf{k}}$) creates (annihilates) a conduction electron with momentum $\mathbf{k}$ and energy $\epsilon_{\mathbf{k}}$ in the left

(L) or the right (R) lead, ω_0 is the vibrational frequency of the molecule, and $\mathbf{a}^{\dagger}$ ($\mathbf{a}$) is the phonon creation (annihilation) operator. The third term $\mathbf{H}_D$ describes the coupling between the SMT electron and local phonon mode with strength λ,

$$\mathbf{H}_{\text{D}} = \left[\epsilon_0 + \lambda \left(\mathbf{a} + \mathbf{a}^{\dagger} \right) \right] \mathbf{d}^{\dagger} \mathbf{d}, \tag{3}$$

where $\mathbf{d}^{\dagger}$ ($\mathbf{d}$) is the corresponding creation (annihilation) operator of the SMT or QD electron associated with the energy ϵ_0. The last term $\mathbf{H}_T$ describes the hopping of electron between the SMT and leads with the tunnelling matrix elements denoted as $V_{\mathbf{k}}$,

$$\mathbf{H}_T = \sum_{\mathbf{k} \in L(R)} \left[V_{\mathbf{k}} \mathbf{c}_{\mathbf{k}}^{\dagger} \mathbf{d} + \text{h.c.} \right]. \tag{4}$$

The chemical potentials in the left and right lead are denoted by $\mu_{L(R)}$, respectively, which are related to the bias, V_{bias}, and the average of two lead potentials, V_{mid}, through $V_{bias} = (\mu_L - \mu_R)/e$ and $V_{mid} \equiv (\mu_L + \mu_R)/2e$. By changing the external bias and gate voltages experimentally, $\mu_{L(R)}$ and ϵ_0 can be adjusted independently.

In the strong EPI regime, it is appropriate to eliminate the electron-phonon coupling terms in the Hamiltonian by using a nonperturbative canonical transformation, i.e., $\overline{\mathbf{H}} = e^{\mathbf{S}} \mathbf{H} e^{-\mathbf{S}}$ with $\mathbf{S} = \frac{\lambda}{\omega_0} \mathbf{d}^{\dagger} \mathbf{d} \left(\mathbf{a}^{\dagger} - \mathbf{a} \right)$. The transformed Hamiltonian reads $\overline{\mathbf{H}} = \overline{\mathbf{H}}_{\text{ph}} + \overline{\mathbf{H}}_{\text{el}}$, where the phonon part keeps unchanged, while the electron part is reshaped into

$$\overline{\mathbf{H}}_{el} = \sum_{\mathbf{k}} \epsilon_{\mathbf{k}} \mathbf{c}_{\mathbf{k}}^{\dagger} \mathbf{c}_{\mathbf{k}} + \tilde{\epsilon}_0 \mathbf{d}^{\dagger} \mathbf{d} + \sum_{\mathbf{k}} \left[\widetilde{V}_{\mathbf{k}} \mathbf{c}_{\mathbf{k}}^{\dagger} \mathbf{d} + \text{h.c.} \right]. \tag{5}$$

It is clear that due to the EPI, the energy level of SMT is renormalized to $\tilde{\epsilon}_0 \equiv \epsilon_0 - g\omega_0$, where $g \equiv (\lambda/\omega_0)^2$, and the dressed tunnelling matrix elements are transformed into $\widetilde{V}_{\mathbf{k}} \equiv V_{\mathbf{k}} \mathbf{X}$, where the phonon operator $\mathbf{X} \equiv \exp \left[- (\lambda/\omega_0) \left(\mathbf{a}^{\dagger} - \mathbf{a} \right) \right]$ arises from the canonical transformation of the particle operator $e^{\mathbf{S}} \mathbf{d} e^{-\mathbf{S}} = \mathbf{d} \mathbf{X}$. This reveals that the interaction between the SMT electron and the local phonon mode results in an effective phonon-mediated coupling between the SMT and the lead electrons. As in dealing with the localized polaron[28,29], here it is reasonable to replace the operator $\mathbf{X}$ with its expectation value $\langle \mathbf{X} \rangle$, i.e., $\widetilde{V}_{\mathbf{k}} = V_{\mathbf{k}} \exp \left[-g \left(N_{ph} + 1/2 \right) \right]$, where N_{ph} is the phonon population, and can be expressed as $N_{ph} = 1/ \left[\exp \left(\beta \omega_0 \right) - 1 \right]$ with $\beta = 1/k_B T$. Notice that this is an important approximation made in the present paper, which is valid only when the hopping is small compared to the EPI, i.e. $V_{\mathbf{k}} \ll \lambda$.

B. Formalism

By using the Keldysh Green's function technique[26,27,28], the current through an interaction region coupled to two leads can be expressed

as[30,31],

$$J = \frac{ie}{2h} \int d\omega \left\{ \left[f_L(\omega) \Gamma^L - f_R(\omega) \Gamma^R \right] (G^r(\omega) - G^a(\omega)) \right.$$
$$\left. + \left(\Gamma^L - \Gamma^R \right) G^<(\omega) \right\}, (6)$$

where $f_{L(R)}$ is the Fermi distribution function in the left (right) lead, $\Gamma^{L(R)}(\epsilon) \equiv 2\pi\rho_{L(R)}(\epsilon) |V_{L(R)}(\epsilon)|^2$, $\rho_{L(R)}(\epsilon)$ is the density of states in the left (right) lead, $V_{L(R)}(\epsilon)$ equals $V_{\mathbf{k} \in L(R)}$ for $\epsilon = \epsilon_{\mathbf{k}}$, and $G^{r(a)}(\omega)$, $G^<(\omega)$ are the Fourier transformations of the standard Keldysh retarded (advanced) and lesser Green functions for the dot electron, respectively[28]. To note that the parameters $\Gamma_{L(R)}$ are not the renormalized ones, because derivation of this current formula only relies on the hopping terms, regardless the nature of the interacting region. In calculating the current, one needs the spectral function, which is defined as

$$A(\omega) = i\left(G^r(\omega) - G^a(\omega) \right) = i\left(G^>(\omega) - G^<(\omega) \right), \quad (7)$$

and the lesser Green's function $G^<$, which is proportional to spectral function and the occupation of the electron.

When the operator $\mathbf{X}$ is replaced by its expectation value, the Hamiltonian Eq.(5) is decoupled from the phonon operator, then the interacting lesser Green function may be separated:

$$G^<(t) \equiv i\left\langle \mathbf{d}^\dagger(0)\mathbf{d}(t) \right\rangle = i\left\langle \overline{\mathbf{d}}^\dagger e^{i\overline{\mathbf{H}}t}\overline{\mathbf{d}}e^{-i\overline{\mathbf{H}}t} \right\rangle$$
$$= i\left\langle \mathbf{d}^\dagger e^{i\overline{\mathbf{H}}_{el}t}\mathbf{d}e^{-i\overline{\mathbf{H}}_{el}t} \right\rangle_{el} \left\langle \mathbf{X}^\dagger e^{i\overline{\mathbf{H}}_{ph}t}\mathbf{X}e^{-i\overline{\mathbf{H}}_{ph}t} \right\rangle_{ph}$$
$$\equiv \widetilde{G}^<(t) e^{-\Phi(-t)}, \quad (8)$$

and similarly,

$$G^>(t) \equiv -i\left\langle \mathbf{d}(t)\mathbf{d}^\dagger(0) \right\rangle = \widetilde{G}^>(t) e^{-\Phi(t)}, \quad (9)$$

where $\widetilde{G}^{>(<)}(t)$ is the dressed greater (lesser) Green function for a dressed SMT electron governed by $\overline{\mathbf{H}}_{el}$, and the factor $e^{-\Phi(\mp t)}$ arises from the trace of the phonon parts $\left\langle \mathbf{X}^\dagger(0)\mathbf{X}(t) \right\rangle_{ph}$ or $\left\langle \mathbf{X}(t)\mathbf{X}^\dagger(0) \right\rangle_{ph}$, respectively,[28]

$$\Phi(t) = g\left[N_{ph}\left(1 - e^{i\omega_0 t} \right) + (N_{ph}+1)\left(1 - e^{-i\omega_0 t} \right) \right] (10)$$

Note that because $\Phi(-t) \neq \Phi(t)$, the decoupling approximation used in the majority of previous publications,[16,26] which directly decouples the retarded (advanced) Green function as

$$G^{r(a)}(t) = \widetilde{G}^{r(a)}(t) e^{-\Phi(t)}, \quad (11)$$

has ignored the difference between the N_{ph} and $N_{ph}+1$ in the expression of $\Phi(t)$. Although such approximation works well at high temperature, because $N_{ph} \approx N_{ph}+1$, it does make difference at low temperature because of vanishing N_{ph}. We shall further discuss this point latter.
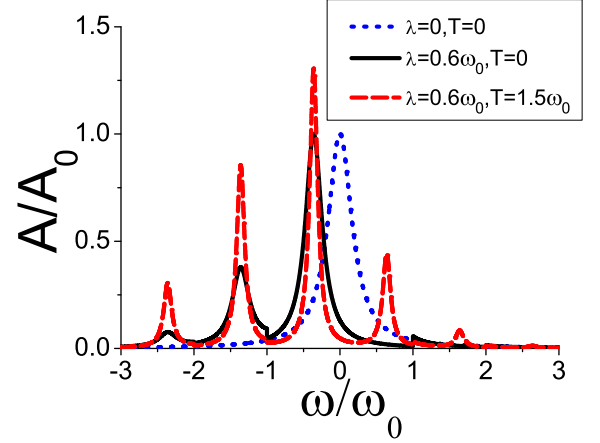

FIG. 2: The dimensionless Spectral function of the SMT electron for different EPI strengths and temperatures. The parameters for calculation are taken as: $\Gamma = 0.2\omega_0$, $\mu_L = \mu_R = \epsilon_0 = 0$, and the unit $A_0 = 2/\Gamma$. The strength of the EPI used here is the same as the references[25].

By using the identity $e^{-\Phi(t)} = \sum_{n=-\infty}^{\infty} L_n e^{-in\omega_0 t}$, the greater and lesser Green functions can be respectively expanded as

$$G^>(\omega) = \sum_{n=-\infty}^{\infty} L_n \widetilde{G}^>(\omega - n\omega_0),$$
$$G^<(\omega) = \sum_{n=-\infty}^{\infty} L_n \widetilde{G}^<(\omega + n\omega_0), \quad (12)$$

where the index n stands for the number of phonons involved, and L_n are the coefficients depending on temperature and the strength of EPI. At finite temperature,

$$L_n \equiv e^{-g(2N_{ph}+1)} e^{n\omega_0\beta/2} I_n\left(2g\sqrt{N_{ph}(N_{ph}+1)} \right), (13)$$

where $I_n(z)$ is the n-th Bessel function of complex argument. At zero temperature, L_n simply reads

$$L_n \equiv \begin{cases} e^{-g}\frac{g^n}{n!} & n \geq 0 \\ 0 & n < 0 \end{cases} \quad (14)$$

Thus the spectral function can be expressed as

$$A(\omega) = \sum_{n=-\infty}^{\infty} iL_n\left[\widetilde{G}^>(\omega - n\omega_0) - \widetilde{G}^<(\omega + n\omega_0) \right] (15)$$

With the help of the equation of motion approach, the retarded (advanced) Green function for the dressed electron can be analytically evaluated as

$$\widetilde{G}^{r(a)}(\omega) = \frac{1}{\omega - \widetilde{\epsilon}_0 - \widetilde{\Sigma}^{r(a)}(\omega)}, \quad (16)$$

where the retarded (advanced) self-energy is

$$\widetilde{\Sigma}^{r(a)}(\omega) = \sum_{k \in L, R} \frac{|\widetilde{V}_k|^2}{\omega - \epsilon_k \pm i\eta} = \widetilde{\Lambda}(\omega) \mp i\widetilde{\Gamma}(\omega). \quad (17)$$

For simplicity, in the wide-band limit, both the real and the imaginary part of the self-energy, $\widetilde{\Lambda}(\omega)$, and $\widetilde{\Gamma}(\omega)$, are assumed to be constants independent of energy. Thus, when the real part of the self-energy is absorbed into the SMT level shift, only the broadening due to the tunnel coupling will be considered. With the assumption of symmetric coupling, $\widetilde{\Gamma}^L \approx \widetilde{\Gamma}^R = \widetilde{\Gamma}$, the broadening can be expressed as $\widetilde{\Gamma}(\omega) = (\widetilde{\Gamma}^L + \widetilde{\Gamma}^R)/2 = \widetilde{\Gamma}$. Then the spectral function of the dressed SMT electron can be cast into

$$\widetilde{A}(\omega) = \frac{2\widetilde{\Gamma}}{(\omega - \widetilde{\epsilon}_0)^2 + \widetilde{\Gamma}^2}. \quad (18)$$

Following the Keldysh equation[27] for the lesser Green function, i.e., $\widetilde{G}^<(\omega) = \widetilde{G}^r(\omega)\widetilde{\Sigma}^<(\omega)\widetilde{G}^a(\omega)$ with $\widetilde{\Sigma}^<(\omega) = i\widetilde{\Gamma}(f_L(\omega) + f_R(\omega))$, the relation between the dressed greater or lesser Green function and the dressed spectral function is respectively as

$$\widetilde{G}^>(\omega) = -i\frac{2 - f_L(\omega) - f_R(\omega)}{2}\widetilde{A}(\omega),$$

$$\widetilde{G}^<(\omega) = i\frac{f_L(\omega) + f_R(\omega)}{2}\widetilde{A}(\omega). \quad (19)$$

Thus the spectral function of the SMT electron $A(\omega)$ can readily be obtained by substituting Eqs.(19) and (18) into Eq.(15).

III. THE SPECTRAL FUNCTION OF THE SMT ELECTRON

A. The dressing effects caused by the EPI

The spectral function for our structure generally depends on the EPI strength, temperature, and chemical potential in two leads relative to the SMT level. Let us first address the first two dependencies in the case of $\mu_L = \mu_R = \epsilon_0$.

As plotted in Fig.2, the effect of the EPI and temperature on the spectral functions of the SMT electron are evaluated. For comparison, the spectral function without the EPI at $0K$ is also shown, which exhibits a single resonant peak at ϵ_0 with a Lorentzian. Compared with the EPI-free case, with finite EPI, the resonant peak at ϵ_0 in the spectral function is red-shifted by $g\omega_0$, and the spectral peak is sharpened. This results from the renormalized effects on the SMT level and the dressing effect on the tunnelling matrix elements $V_{\mathbf{k}}$ due to the EPI. More noticeably, new satellite peaks may appear at $\widetilde{\epsilon}_0 \pm n\omega_0$ in the spectral function, implying that due to the EPI the ground state for the coupled system may possess finite components involving n phonons. For later convenience,
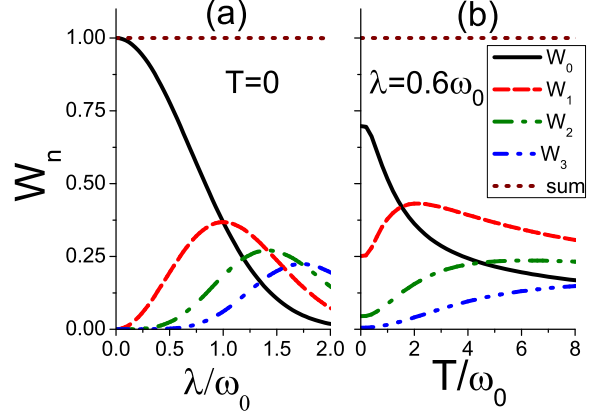

FIG. 3: The total weights of the $+n$-th and the $-n$-th phonon sidebands, W_n, as functions of the (a) strength of EPI λ and (b) temperature T, where $\Gamma = 0.2\omega_0$, while $\mu_{L(R)}$ are arbitrary. The dot lines are the numerical summation, $\sum_n W_n$.

we label the resonant peak located at $\widetilde{\epsilon}_0$ as the zero-phonon-band, and the satellite peaks located at $\widetilde{\epsilon}_0 \pm n\omega_0$ as the $\pm n$-th phonon sidebands. In general, these phonon sidebands are not symmetric with respect to $\widetilde{\epsilon}_0$. By using the identity

$$i\int_{-\infty}^{\infty} d\omega(\widetilde{G}^>(\omega - n\omega_0) - \widetilde{G}^<(\omega + n\omega_0))$$

$$= i\int_{-\infty}^{\infty} d\omega(\widetilde{G}^>(\omega) - \widetilde{G}^<(\omega)) = 2\pi, \quad (20)$$

and $\sum_{n=-\infty}^{\infty} L_n = \exp\{\Phi(0)\} = 1$, it can be seen that the sum rule for the spectral function still holds in the presence of EPI, namely

$$\int_{-\infty}^{\infty} d\omega A(\omega) = 2\pi. \quad (21)$$

As shown in Fig.2, the weight of each peak, defined as the integrated area under the peak divided by 2π and denoted by $W_{\pm n}$, is sensitive to the EPI strength and temperature. We can further define sum of the spectral weights of the $+n$-th and $-n$-th phonon sidebands as

$$W_n \equiv W_{+n} + W_{-n} = L_n + L_{-n} = e^{-g(2N_{ph}+1)}$$

$$\times \left(e^{n\omega_0\beta/2} + e^{-n\omega_0\beta/2}\right)I_n\left(2g\sqrt{N_{ph}(N_{ph}+1)}\right) \quad (22)$$

Fig.3 shows that when λ or T increases, the spectral weight of the zero-phonon band, W_0 decreases monotonically; while the phonon sideband, $W_n(n \neq 0)$, gets lager first, then reaches a maximum value for a certain EPI strength or temperature, and decreases again. This reflects that when increasing the temperature or EPI strength, the occupation probability of the phonon sideband increases, keeping the conservation of the total
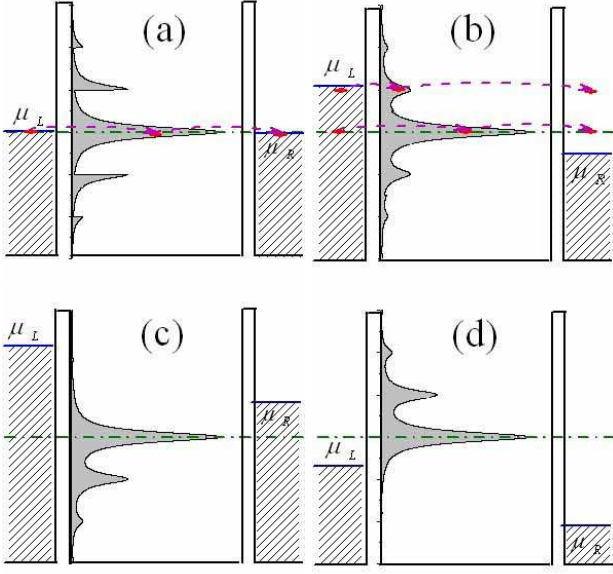
FIG. 4: The spectral functions of the SMT electron for four typical configurations of $\mu_{L(R)}$: (a) $\mu_L = \mu_R = \widetilde{\epsilon}_0$, (b) $\mu_L = \widetilde{\epsilon}_0 + 0.9\omega_0, \mu_R = \widetilde{\epsilon}_0 - 0.5\omega_0$, (c) $\mu_L = \widetilde{\epsilon}_0 + 2.2\omega_0, \mu_R = \widetilde{\epsilon}_0 + 0.8\omega_0$, (d) $\mu_L = \widetilde{\epsilon}_0 - 0.8\omega_0, \mu_R = \widetilde{\epsilon}_0 - 2.2\omega_0$, where the parameters are $\Gamma = 0.2\omega_0$, $\lambda = 0.6\omega_0$, $T = 0$ and $\widetilde{\epsilon}_0 = 0$. The balls connected by the dash lines in (a) and (b) denote the resonant tunnelling processes for electrons.

spectral weight, *i.e.*, $\sum_{n=0}^{\infty} W_n = 1$. Note that these variation trends are not in contradiction with Fig.2, where the heights of both the zero-phonon peak and phonon sidebands increase as temperature gets higher, as the corresponding widths are narrowed simultaneously.

B. The interplay between the EPI and the SMT electron-lead coupling

Now let us take a close look at the dependence of the spectral function of the SMT electron on the chemical potentials in two leads in the presence of the EPI.

As shown in Fig.4, it is quite interesting that the spectral function of the SMT electron profiles quite differently for the same EPI strength and temperature ($0K$), but under different configurations of the chemical potentials in two leads. And the phonon sidebands, whose lineshapes may vary abruptly at certain frequency, can be nonvanishing in both sides of the zero-phonon band, even at zero temperature. This is quite different from the usual Independent Boson Model, according to which, the phonon sidebands have nothing to do with the lead chemical potentials, and at zero temperature, they should vanish on the negative energy side of the zero-phonon band of the hole.

The unusual behavior of the present spectral function can be understood with Eqs.(15) and (19), in which $\widetilde{G}^{>}(\omega - n\omega_0)$, and $\widetilde{G}^{<}(\omega + n\omega_0)$ in general depends on

the Fermi function of $f_L(f_R)$ in the left (right) lead, and thus on the chemical potential, $\mu_L(\mu_R)$, respectively. At zero temperature, the expansion coefficients L_n vanish for negative n, therefore only the zero-phonon band of the spectral function can both the lesser and greater Green function contribute to; while the phonon sideband below the zero-phonon band results from the $\widetilde{G}^{<}(\omega + n\omega_0)$, and that above the zero-phonon band comes from the $\widetilde{G}^{>}(\omega - n\omega_0)$.

Recalling that the lesser and greater Green functions $\widetilde{G}^{<(>)}$ correspond to the dressed SMT electron and hole propagator, which are proportional to the occupation number, n_{SMT}, for the SMT electron, or $1 - n_{SMT}$ for the hole, respectively. Different from the Independent Boson Model, where n_{SMT} is fixed to either zero or one at $0K$, as the Fermi level for the isolate system is well defined, in the present non-equilibrium model, due to the tunnelling coupling the occupation of the SMT electron is determined by the chemical potentials at the left and right leads when the system approaches a steady state. Thus, by tuning the lead chemical potentials, n_{SMT} can take any value between zero and one, consequently, even at $0K$ the contribution from both the electron and hole to the spectral function of the SMT need considering. At low temperature the SMT electron and hole can only emit phonons, so the phonon sidebands below the zero-phonon band come from the occupative SMT electron, while those above the zero-phonon band originate from the SMT hole. If there is a partial occupation in the zero-phonon band for the SMT electron, it is required to carefully examine the contribution from both electron and hole. It is the different treatment of n_{SMT} that leads to the unusual behavior of the phonon sidebands at zero temperature.

The spectral function can be explicitly expressed as functions of the bias and V_{mid}, the average of two lead potentials relative to the renormalized SMT level as defined in the Section II, *i.e.*, $A(\omega, V_{mid}, V_{bias})$. In this way the effect due to the bias and due to the V_{mid} on the spectral function will be considered separately. We have found that the V_{mid} mostly affects the lineshape of the spectral function in the present model. Four typical configurations of the lead chemical potentials in Fig.4 are divided into two categories: (1) The $V_{mid} \sim \widetilde{\epsilon}_0$, namely the SMT level is partially filled. Then for both bias in Fig.4(a) and Fig.4(b), the resonant tunnelling may take place. (2) The V_{mid} deviates from $\widetilde{\epsilon}_0$ significantly compared with the band-width $\widetilde{\Gamma}$, so that the SMT level is either fully occupied or totally empty, *i.e.* $n_{SMT} \simeq 1$ (Fig.4(c)), or $n_{SMT} \simeq 0$ (Fig.4(d)), in which no resonant tunnelling can occur.

In Fig.4(a), both chemical potentials in the leads align exactly with the renormalized SMT level, where and the lineshape of each phonon sideband exhibits discontinuity at certain frequency. This is similar to the case $\mu_L = \mu_R = \epsilon_0$ (*cf.* Fig.2), except for that the spectral function in Fig.4(a) is symmetric with respect to $\widetilde{\epsilon}_0$, while that in Fig.2 is asymmetric. This is understandable, be-

cause at zero bias and zero temperature there exist a well-defined boundary, $\mu_L = \mu_R$, separating the SMT electron from hole. The symmetric spectral function is an exception when the renormalized SMT level happens to coincide with the boundary and $n_{SMT} = 0.5$. In Fig.4(b), when the bias is large enough to enclose the most part of the zero-phonon band, both distributions of the SMT electron or hole in the zero-phonon band become Lorenzian, and so does the lineshape of each phonon sideband. Strictly speaking, the spectral function in Fig.4(b) is not symmetric around $\widetilde{\epsilon}_0$ as $V_{mid} \neq \widetilde{\epsilon}_0$, but the asymmetric part can be hardly discerned for the present case. It is noticed that whenever one of the phonon sidebands enters the bias region, there will be the phonon-assisted tunnelling process. Compare Fig.4(b) to (a), it is evident that the bias is not only important in determining the profile of each phonon sideband, but also crucial in controlling the phonon-assisted tunnelling. It is interesting to observe that when $n_{SMT} \simeq 0$ (Fig.4(d)), which corresponds to the one-hole picture, the usual result following the Independent Boson Model with one hole[28] is recovered; on the other hand, when $n_{SMT} \simeq 1$ as in Fig.4(c), which corresponds to the picture of one-electron, the spectral function is reversed with respect to $\widetilde{\epsilon}_0$ compared with (d). Comparison among the four configurations shows that the V_{mid} relative to $\widetilde{\epsilon}_0$ has played a decisive role in determining the occupation of the SMT level, or equivalently the partition between the SMT electron and hole.

The spectral function has been found to have the symmetry as follows,

$$A(\omega, V_{mid}, -V_{bias}) = A(\omega, V_{mid}, V_{bias}), \qquad (23)$$

and

$$A(\omega = \widetilde{\epsilon}_0 - \Delta\omega, V_{mid} = \widetilde{\epsilon}_0/e - \Delta V, V_{bias})$$
$$= A(\omega = \widetilde{\epsilon}_0 + \Delta\omega, V_{mid} = \widetilde{\epsilon}_0/e + \Delta V, V_{bias}). \qquad (24)$$

Compared to the EPI-free case, the spectral function in the EPI is generally asymmetric with respect to $\widetilde{\epsilon}_0$ unless $eV_{mid} = \widetilde{\epsilon}_0$. This implies a broken electron-hole symmetry, which can also be seen from Fig.4, where the spectral function in (a) is symmetric with respect to $\widetilde{\epsilon}_0$; while in Fig.4 (b), (c) and (d), there are broken symmetry for electron and hole, particularly obvious for cases of (c) and (d).

With increasing temperature, one can expect that the profile of the dot spectral function should be less and less sensitive to the variation of the lead chemical potentials, because the Fermi distribution varies continuously across $\mu_{L(R)}$ at high temperature, so do the phonon sidebands.

IV. THE TRANSPORT PROPERTIES

Based on the spectral function discussed above, in this section, we shall investigate the differential conductance and tunnelling current of the SMT(QD) system. The case of zero temperature will be discussed first, then follows the modifications by the finite temperature effect.

A. The zero temperature

At zero temperature, the Fermi distribution functions are the step functions $\Theta(\mu_{L(R)} - \omega)$, and the coefficients L_n reduce to the Eq.14, thus the current can be expressed explicitly as

$$J = \frac{e}{4h} \sum_{n=0}^{\infty} L_n \Gamma \int d\omega \left[\Theta\left(\mu_L - \omega\right) - \Theta\left(\mu_R - \omega\right)\right] \left\{ \left[\Theta\left(\mu_L - \omega - n\omega_0\right) + \Theta\left(\mu_R - \omega - n\omega_0\right)\right]\widetilde{A}(\omega + n\omega_0) \right.$$
$$\left. + \left[2 - \Theta\left(\mu_L - \omega + n\omega_0\right) - \Theta\left(\mu_R - \omega + n\omega_0\right)\right]\widetilde{A}(\omega - n\omega_0) \right\}. \qquad (25)$$

Using $\mu_{L(R)} = eV_{mid} \pm eV_{bias}/2$, and $\partial\Theta(\mu_{L(R)} - \omega)/\partial V_{bias} = \pm e\delta(\mu_{L(R)} - \omega)/2$, the differential conductance can be obtained by performing $\partial J/\partial V_{bias}$,

$$G(V_{mid}, V_{bias}) = \frac{e^2}{8h} \sum_{n=0}^{\infty} L_n \Gamma \left\{ \Theta(eV_{bias} - n\omega_0) \left[\widetilde{A}(\mu_L) + \widetilde{A}(\mu_R) + \widetilde{A}(\mu_L - n\omega_0) + \widetilde{A}(\mu_R + n\omega_0)\right] \right.$$
$$\left. + \Theta(-eV_{bias} - n\omega_0) \left[\widetilde{A}(\mu_L) + \widetilde{A}(\mu_R) + \widetilde{A}(\mu_L + n\omega_0) + \widetilde{A}(\mu_R - n\omega_0)\right] \right\}. \qquad (26)$$
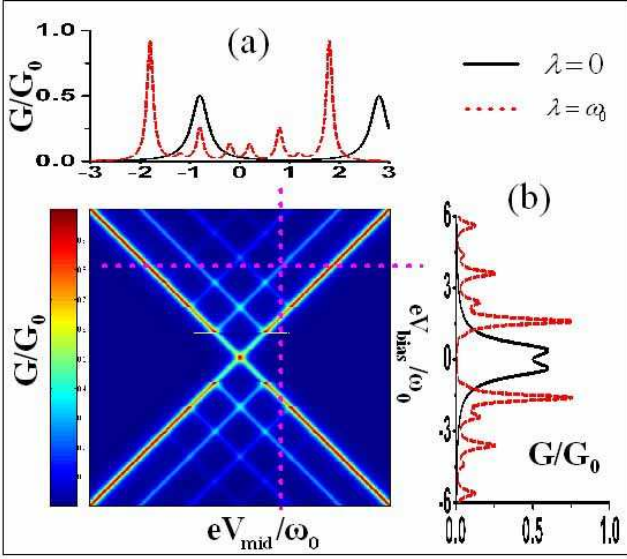
FIG. 5: (Color on line) The dimensionless differential conductance ($G_0 = e^2/2h$) at $T = 0K$ as functions of V_{mid} and V_{bias}. The parameters for calculation are taken as: $\Gamma = 0.2\omega_0$, $\epsilon_0 = \omega_0$, and $\widetilde{\epsilon}_0 = 0$ which implies that for the sake of clarity a stronger EPI strength, $\lambda = \omega_0$, is chosen. The color scale runs from zero (blue) to G_0 (red). The above (a) and right (b) panels to the map are the sections for a fixed value of $eV_{bias}^{fix} = 3.6\omega_0$ and $eV_{mid}^{fix} = 0.8\omega_0$, respectively, marked on the map with dash lines.

It is easy to verify that the tunnelling current and differential conductance satisfy the symmetry relations as

$$J(V_{mid} = \widetilde{\epsilon}_0/e - \Delta V, V_{bias}) = J(V_{mid} = \widetilde{\epsilon}_0/e + \Delta V, V_{bias}),$$
$$G(V_{mid} = \widetilde{\epsilon}_0/e - \Delta V, V_{bias}) = G(V_{mid} = \widetilde{\epsilon}_0/e + \Delta V, V_{bias}),$$

and

$$\begin{aligned} J(V_{mid}, -V_{bias}) &= -J(V_{mid}, V_{bias}), \\ G(V_{mid}, -V_{bias}) &= G(V_{mid}, V_{bias}). \end{aligned} \quad (27)$$

It is noticed that due to the equivalence between the current of electron type and hole type, the broken symmetry with respect to $\widetilde{\epsilon}_0$ in the spectral function of SMT electron is now restored for the tunnelling current and differential conductance.

The map plotted in Fig.5 is the calculated differential conductance as function of V_{mid} and V_{bias} in the presence of the EPI. The dashed lines in Fig.5(a) and (b) represent the differential conductance for a fixed value of $eV_{bias}^{fix} = 3.6\omega_0$ and $eV_{mid}^{fix} = 0.8\omega_0$, respectively; while the solid lines correspond to the differential conductance without the EPI as for reference, in which the peaks appear only when one of the lead chemical potentials is aligned with the SMT level, i.e., $\mu_L(\mu_R) = \epsilon_0$. Compared with the EPI-free case, the corresponding peaks in the presence of finite EPI are sharpened, and red-shifted by $g\omega_0$, and more noticeably, new satellite peaks are shown up, which are associated with the phonon-assisted tunnelling processes as depicted in Fig.4(b),
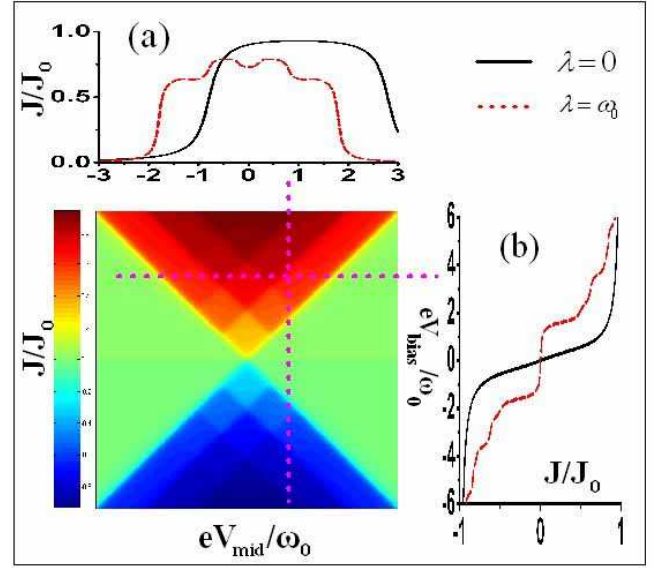

FIG. 6: (Color on line) The map of tunnelling current, $J(V_{mid}, V_{bias})$, at $T = 0K$, where the parameters are taken as the same as the Fig.5, and $J_0 = e\Gamma/2\hbar$. The color scale runs from $-0.9J_0$ (blue) to $0.9J_0$ (red). The solid and dashed lines in sections (a) and (b) represent the tunnelling current for the cases without and with EPI, respectively.

when $\mu_L = \widetilde{\epsilon}_0 + n\omega_0$ or $\mu_R = \widetilde{\epsilon}_0 - n\omega_0$ for $V_{bias} \geq 0$; $\mu_L = \widetilde{\epsilon}_0 - n\omega_0$ or $\mu_R = \widetilde{\epsilon}_0 + n\omega_0$ for $V_{bias} < 0$, where $n \leq \Theta(|eV_{bias}|/\omega_0)$.

The map plotted in Fig.6 is the tunnelling current as function of V_{mid} and V_{bias}, which can be divided into several plateaus with the bounded lines corresponding to the differential conductance peaks in Fig.5. It should be pointed out that the phonon-assisted tunnelling can take place even at zero temperature. Although no thermal phonon is available at $0K$, the phonon-emitted process accompanying the tunnel is possible, if the phonon energy can be supplied by the bias voltage across the SMT. As also shown in the map (Fig.5), the phonon-assisted peaks are absent in the left and right quarters, which are bounded by the lines of the zero-phonon peaks.

Now let us discuss the relationship between the transport properties and the SMT spectral function. As mentioned above, due to the dressing effects of EPI, the SMT electron still has a finite probability to occupy the phonon sidebands even at zero temperature. Once a phonon sideband of the SMT enters the bias region, the phonon-assistant-channel would be open, as depicted in Fig.4(b). Thus the information of the SMT spectral function can be inferred from the spectra of the tunnelling current or differential conductance. For example, for a fixed V_{mid}, the integral of the differential conductance over V_{bias} satisfies a sum rule, $\int_{-\infty}^{\infty} dV_{bias} G(V_{mid}, V_{bias}) = J_0$, which just results from the conservation of the spectral weights in Eq.(21). While for a fixed V_{bias}, the integral of the differential conductance over V_{mid} does not equal J_0 in consequence of the transfer of a finite spectral weights
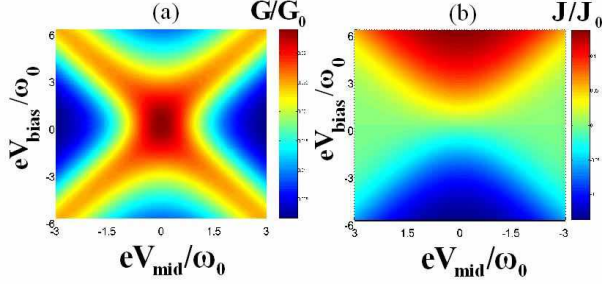
FIG. 7: (Color on line) The dimensionless differential conductance and tunnelling current as functions of V_{mid} and V_{bias}, (a) $G(V_{mid}, V_{bias})$, (b) $J(V_{mid}, V_{bias})$, where $\Gamma = 0.2\omega_0$, $\lambda = \omega_0$, $T = 0.6\omega_0$, $\widetilde{\epsilon}_0 = 0$, and the units $G_0 = e^2/2h$, $J_0 = e\Gamma/2\hbar$. The color scale runs from zero conductance (blue) to $0.05G_0$ (red) in (a) and from $-0.15J_0$ (blue) to $0.15J_0$ (red) in (b).

to those phonon sidebands, which do not participate in tunnelling. This is a little different from the tunnelling process without the EPI, where the sum rule for the differential conductance always holds.

We will end this subsection with a comparison between the results based on different decoupling approximations, i.e., Eq.(9) and Eq.(11). In the zero bias limit, by using Eq.(9), the differential conductance would have no phonon-assisted peaks as clearly shown in Fig.5. On the other hand, by following Eq.(11), there would be a set of non-vanishing phonon-assisted peaks in the differential conductance[15,16,26,28,30]. This discrepancy can be explained in terms of the different SMT spectral functions obtained in different approximations. Once the

Green function is decoupled according to Eq.(11), the SMT spectral function would be expanded in the following way,

$$B(\omega) = \sum_{n=-\infty}^{\infty} L_n \left[\widetilde{A}(\omega - n\omega_0) \right]. \qquad (28)$$

At zero temperature, we have $n \geq 0$, the profile of $B(\omega)$ is similar to Fig.4(d), namely there is a set of non-vanishing phonon sidebands above the zero-phonon band, which is independent of the Fermi distributions in the leads. Thus, following the approximation (11), in the zero bias limit, the differential conductance would exhibit a set of phonon peaks. Physically, our results which follow Eqs. (9) and (8), seem more reasonable, because the tunnelling electron can neither absorb nor emit any phonon in the zero temperature and zero bias limit.

B. finite temperature

The tunnelling current at finite temperature can readily be obtained from Eq.(6). With the help of the identities $L_{-n} = e^{-\beta n\omega_0} L_n$ and $\partial f_{L(R)}(\omega)/\partial V_{bias} = \pm e\beta f_{L(R)}(\omega)(1 - f_{L(R)}(\omega))/2$, the differential conductance can be expressed in a compact form:

$$G = \frac{e^2\Gamma}{2h} \sum_{n=-\infty}^{\infty} L_n \int_{-\infty}^{\infty} d\omega F_n(\omega) \widetilde{A}(\omega - n\omega_0), \quad (29)$$

where the factors $F_n(\omega)$ depend on the Fermi distributions in the leads through,

$$F_n(\omega) = \frac{\beta}{2} \left\{ [f_L(\omega)(1 - f_L(\omega)) + f_R(\omega)(1 - f_R(\omega))][1 + \frac{e^{-\beta n\omega_0} - 1}{2}(f_L(\omega - n\omega_0) + f_R(\omega - n\omega_0))] \right.$$
$$\left. + \frac{e^{-\beta n\omega_0} - 1}{2}(f_L(\omega) - f_R(\omega))[f_L(\omega - n\omega_0)(1 - f_L(\omega - n\omega_0)) - f_R(\omega - n\omega_0)(1 - f_R(\omega - n\omega_0))] \right\}. (30)$$

Both maps for the differential conductance and tunnelling current at finite temperature are plotted in Fig.7. Compared to the zero temperature case, the differential conductance peaks at finite temperature are broadened and smeared out to some extent, and the tunnelling current profile become smoother and less sensitive to the bias, which results from the smoother Fermi distributions in the leads at finite temperature. Moreover, since the phonon sidebands of the spectral function will distribute more symmetrically around the zero-phonon-peak at finite temperature than the $0K$ case as shown in Fig.2, the phonon-assisted peaks of the differential conductance might appear in the two forbidden quarters as shown in Fig.5 at $0K$. Therefore, the difference caused by the dif-

ferent decoupling approximations as discussed above will be diminished with increasing the temperatures.

V. CONCLUSION

In summary, we have theoretically studied the non-equilibrium quantum transport through the single molecule transistor or quantum dot in the presence of the local electron-phonon interaction. Owing to the EPI, the spectral function of the dot electron will manifest itself in the phonon-dressing effects, such as the red-shift and sharpening of the zero phonon peak, and the transfer of finite spectral weights to the phonon sidebands. Fur-

thermore, due to the interplay between the EPI and the dot-lead coupling, the zero-phonon band and the phonon sidebands of the spectral function at low temperature critically depend on the chemical potentials at two leads and can thus be manipulated. Although the sum of the spectral weights for the $+n$-th and $-n$-th phonon sideband is fixed for a given temperature and EPI strength, the distribution of the spectral weights is dependent on the chemical potentials in two leads, in particular on the average of two lead potentials relative to the renormalized SMT level, showing the broken electron-hole symmetry. The tunnelling current and differential conductance have been analyzed at both zero and finite temperatures, which also reveal the dependence on the chemical potentials of the leads. Different approximations used in decoupling the electron-phonon system have been compared and discussed. It has been found that although different decoupling approximations can yield nearly the same results at high temperature, they do lead to quite different behaviors at zero temperature.

* Electronic address: zzchen@castu.tsinghua.edu.cn

† Electronic address: bfzhu@castu.tsinghua.edu.cn

[1] J. Reichert, R. Ochs, D. Beckmann, H.B. Weber, M. Mayor, and H.v. Lhneysen, Phys. Rev. Lett. **88**, 176804 (2002).

[2] H. Park, J. Park, A.K.L. Lim, E.H. Anderson, A.P. Alivisatos, and P.L. McEuen, Nature (London) **407**, 57 (2000).

[3] J. Park, A. Pasupathy, J. Goldsmith, C. Chang, Y. Yaish, J. Petta, M. Rinkoski, J. Sethna, H. Abruna, and P. McEuen, Nature (London) **417**, 722 (2002).

[4] W. Liang, M. Shores, M. Bockrath, J. Long, and H. Park, Nature **417**, 725 (2002).

[5] S. Kubatkin, A. Danilov, M. Hjort, J. Cornil, J.-L. Brédas, N. Stuhr-Hansen, P. Hegård, and T. Bjφrnholm, Nature **425**, 698 (2003).

[6] A. N. Pasupathy, R. C. Bialczak, J. Martinek, J. E. Grose, L. A. K. Donev, P. L. McEuen, and D. C. Ralph, Science **306**, 86 (2004).

[7] L. H. Yu and D. Natelson, Nanotechnology **15**, S517 (2004).

[8] L. H. Yu and D. Natelson, Nano Letters **4**, 79 (2004).

[9] L. H. Yu, Z. K. Keane, J. W. Ciszek, L. Cheng, M.P. Stewart, J.M. Tour, D. Natelson, Phys. Rev. Lett. **93**, 266802 (2004).

[10] D. Boese and H. Schoeller, Europhys. Lett. 54, 668 (2001); K. D. McCarthy, N. Prokof'ev, and M. T. Tuominen, Phys. Rev. B **67**, 245415 (2003).

[11] A. Mitra, I. Aleiner, A. J. Millis, Phys. Rev. B **69**, 245302 (2004).

[12] J. Koch and F. V. Oppen, cond-mat/0409667.

[13] N. S. Wingreen, K. W. Jacobsen, and J. W. Wilkins, Phys. Rev. B **40**, 11834 (1989).

[14] A. O. Gogolin and A. Komnik, cond-mat/0207513.

[15] U. Lundin and R. H. McKenzie, Phys. Rev. B **66**, 075303 (2002).

[16] J.-X. Zhu and A. V. Balatsky, Phys. Rev. B **67**, 165326 (2003).

[17] P. S. Cornaglia, H. Ness and D. R. Grempel, Phys. Rev. Lett. **93**, 147201 (2004).

[18] P. S. Cornaglia, D. R. Grempel and H. Ness, Phys. Rev. B **71**, 075320 (2005).

[19] J. Paaske and K. Flensberg, cond-mat/0409158.

[20] A. S. Alexandrov and A. M. Bratkovsky, Phys. Rev. B **67**, 235312 (2003).

[21] K. Flensberg, Phys. Rev. B **68**, 205323 (2003); S. Braig, K. Flensberg, Phys. Rev. B **68**, 205324 (2003).

[22] C. Caroli, R. Combescot, P. Nozieres and D. Saint-Janmes, J. Phys. C: Solid State Physics **5** 21 (1972).

[23] E. V. Anda and F. Flores, J. Phys.: Condens. Matter **3**, 9087 (1991).

[24] M. Galperin and M. A. Ratner, Nanoletters **4**, 1605 (2004).

[25] David M.-T. Kuo and Y. C. Chand, Phys. Rev. B **66**, 085311 (2002).

[26] H. Huag and A. -P. Jauho in *Quantum Kinetics in Transport and Optics of Semiconductors*, edited by Dr. -Ing. Helmut K. V. Lotsch (Springer-Verlag, Berlin Heidelberg, 1996).

[27] D. C. Langreth, in *Linear and Nonlinear Electron Transport in Solids*, edited by J. T. Devreese and V. E. Van Doren (Plenum, New York, 1976).

[28] G. D. Mahan, *Many-Particle Physics*, 3rd ed. (Plenum Press, New York, 2000).

[29] A. Hewson and D. Newns, J. Phys. C **13**, 4477 (1980).

[30] A. -P. Jauho, N. S. Wingreen and Y. Meir, Phys. Rev. B. **50**, 5528 (1994).

[31] Y. Meir and N. S. Wingreen, Phys. Rev. Lett. **68**, 2512 (1992).